Hindawi Publishing Corporation
Bioinorganic Chemistry and Applications
Volume 2006, Article ID 79327, Pages 1–13
DOI 10.1155/BCA/2006/79327

Proposal for Sets of ^{77}Se NMR Chemical Shifts in Planar and Perpendicular Orientations of Aryl Group and the Applications

Satoko Hayashi and Waro Nakanishi

Department of Material Science and Chemistry, Faculty of Systems Engineering, Wakayama University, 930 Sakaedani, Wakayama 640-8510, Japan

Received 18 May 2006; Revised 17 July 2006; Accepted 29 August 2006

The orientational effect of p-YC_6H_4 (Ar) on δ(Se) is elucidated for ArSeR, based on experimental and theoretical investigations. Sets of δ(Se) are proposed for **pl** and **pd** employing 9-(arylselanyl)anthracenes (**1**) and 1-(arylselanyl)anthraquinones (**2**), respectively, where Se–C_R in ArSeR is on the Ar plane in **pl** and perpendicular to the plane in **pd**. Absolute magnetic shielding tensors of Se (σ(Se)) are calculated for ArSeR (R = H, Me, and Ph), assuming **pl** and **pd**, with the DFT-GIAO method. Observed characters are well reproduced by the total shielding tensors (σ^t(Se)). The paramagnetic terms (σ^P(Se)) are governed by $\sigma^P(Se)_{xx} + \sigma^P(Se)_{yy}$, where the direction of n_P(Se) is set to the z-axis. The mechanisms of the orientational effect are established both for **pl** and **pd**. Sets of δ(Se: **1**) and δ(Se: **2**) act as the standards for **pl** and **pd**, respectively, when δ(Se) of ArSeR are analyzed based on the orientational effect.

INTRODUCTION

^{77}Se NMR spectroscopy is one of powerful tools to study selenium compounds [1–20], containing bioactive materials [21–24]. ^{77}Se NMR chemical shifts (δ(Se)) are sharply sensitive to the structural changes in selenium compounds. Therefore, they are widely applied to determine the structures [6–20] and to follow up the reactions of selenium compounds [1–10]. The δ(Se) values have been analyzed variously. The substituent effect is employed when the effect of the electronic conditions around Se on δ(Se) is examined in p-YC_6H_4SeR perturbed by Y, for example [6–20]. Some empirical rules and/or classifications between structures and δ(Se) are proposed [6–20], however, it is not so easy to predict δ(Se) from the structures with substantial accuracy. Some important rules would be behind the observed values. Plain rules, founded on the theoretical background, are necessary to analyze the structures of selenium compounds based on δ(Se) and also to understand the origin of δ(Se) [25].

We have pointed out the importance of the orientational effect on δ(Se) of p-YC_6H_4SeR, for the better understanding of δ(Se) of ArSeR in a uniform manner [19, 20, 25]. To establish the orientational effect, we present two series of δ(Se) for p-YC_6H_4SeR whose structures (conformers) are fixed to planar (**pl**) and perpendicular (**pd**) conformers for all Y examined, under the conditions [26, 27]. (The nonplanar and nonperpendicular conformer (**np**) is also important in some cases, such as the **CC** conformer in 1,8-$(MeZ)_2C_{10}H_6$ (Z = S and Se) [28–33].) (The importance of relative conformations in the substituent effects between substituents and probe sites is pointed out.) The Se−C_R bond in ArSeR is on the Ar plane in **pl** and perpendicular to the plane in **pd**. 9-(Arylselanyl)anthracenes (p-YC_6H_4SeAtc: **1**) and 1-(arylselanyl)anthraquinones (p-YC_6H_4SeAtq: **2**) are the candidates for **pl** and **pd**, respectively: Y in **1** and **2** are H (**a**), NMe_2 (**b**), OMe (**c**), Me (**d**), F (**e**), Cl (**f**), Br (**g**), COOEt (**h**), CN (**i**), and NO_2 (**j**) (see Chart 1). Conformers of the 9-anthracenyl (9-Atc) and 1-anthraquinonyl (1-Atq) groups in **1** and **2** are represented by the type **A** (**A**), type **B** (**B**), and type **C** (**C**) notation, which is proposed for 1-(arylselanyl)naphthalenes (p-YC_6H_4SeNap: **3**) [14–16, 19, 20, 26]. The structure of **1** is **A** for 9-Atc and **pl** for Ar, which is denoted by **1** (**A**: **pl**). That of **2** is **B** for the 1-Atq and **pd** for **Ar** (**2** (**B**: **pd**)). The series of δ(Se) in **1** (δ(Se: **1**)) and δ(Se: **2**) must be typical for **pl** and **pd**, respectively.

Recently, the reliability of the calculated absolute magnetic shielding tensors (σ) is much improved [34–39] and the calculated tensors for Se nuclei (σ(Se)) are demonstrated to

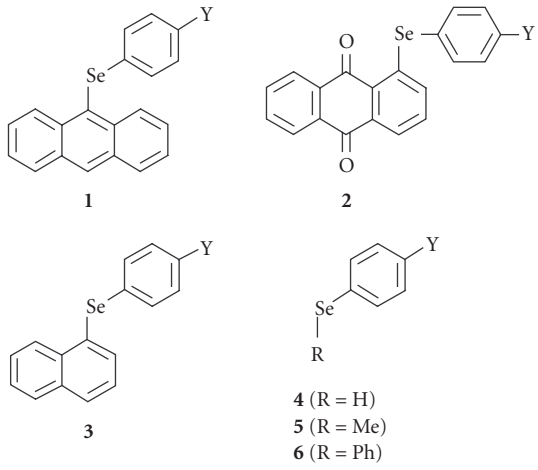

	a	b	c	d	e	f	g	h	i	j
Y =	H	NMe_2	OMe	Me	F	Cl	Br	COOEt	CN	NO_2

Chart 1

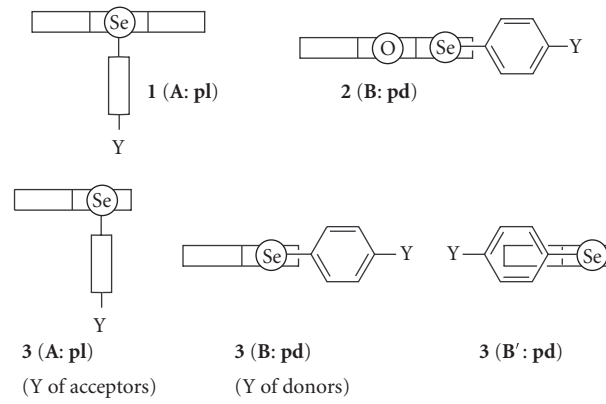

Scheme 1: Structures of **1** and **2**, together with those of **3**.

be useful in usual selenium compounds [28–33].[1] As shown in (1), the total absolute magnetic shielding tensor (σ^t) is decomposed into diamagnetic (σ^d) and paramagnetic (σ^p) contributions [40, 41].[2] σ^p contributes predominantly to σ^t in the structural change of selenium compounds. Magnetic shielding tensors consist of three components, as exemplified by σ^p in (2) as the following:

$$\sigma^t = \sigma^d + \sigma^p, \tag{1}$$

$$\sigma^p = \left(\sigma^p_{xx} + \sigma^p_{yy} + \sigma^p_{zz}\right)/3. \tag{2}$$

Quantum chemical (QC) calculations are performed on ArSeH (**4**), ArSeMe (**5**), and ArSePh (**6**) to understand the orientational effect based on the theoretical background (see Chart 1). The conformations are fixed to **pl** and **pd** in the calculations. The gauge-independent atomic orbital (GIAO) method [42–46] is applied to evaluate σ(Se) at the DFT (B3LYP) level. Mechanisms of the orientational effect are explored for **pl** and **pd** based on the magnetic perturbation theory on the molecules.

After the establishment of the orientational effect of aryl group in p-YC_6H_4SeR, together with the mechanism, δ(Se) of some aryl selenides are plotted versus δ(Se: **1**) and/or δ(Se: **2**). The treatment shows how δ(Se) of aryl selenides are interpreted based on the orientational effect. And it is demonstrated that the sets of δ(Se: **1**) and δ(Se: **2**) give a reliable guideline to analyze the structures of p-YC_6H_4SeR based on δ(Se).

RESULTS

The structures of all members of **1** and **2** are predicted to be **1** (**A**: **pl**) and **2** (**B**: **pd**), respectively [25]. The results are supported by the X-ray crystallographic analysis carried out for **1** and **2**, containing **1c** and **2a** and the QC calculations for **1a** and **2a**, together with the spectroscopic measurements, although not shown. Scheme 1 illustrates **1** (**A**: **pl**) and **2** (**B**: **pd**), together with some conformers of **3**.

Table 1 shows δ(Se: **1**) and δ(Se: **2**), measured in chloroform-d solutions (0.050 M) at 213 K, 297 K, and 333 K.[3] δ(Se: **1a**) and δ(Se: **2a**) are given from MeSeMe and δ(Se: **1**) and δ(Se: **2**) are from **1a** and **2a**, respectively, ($\delta(\text{Se})_{\text{SCS}}$). To examine the temperature dependence in **1**, $\delta(\text{Se: 1})_{\text{SCS}}$ at 297 K ($\delta(\text{Se: 1})_{\text{SCS, 297 K}}$) and $\delta(\text{Se: 1})_{\text{SCS, 333 K}}$ are plotted versus $\delta(\text{Se: 1})_{\text{SCS, 213 K}}$. Table 2 collects the correlations, where the correlation constants (a and b) and the correlation coefficients (r) are defined in the footnote of Table 2 (entries 1 and 2). $\delta(\text{Se: 2})_{\text{SCS, 297 K}}$ and $\delta(\text{Se: 2})_{\text{SCS, 333 K}}$ are similarly plotted versus $\delta(\text{Se: 2})_{\text{SCS, 213 K}}$. Table 2 also contains the correlations (entries 3 and 4). The a values for **1** are smaller than those for **2**. The results show that the temperature dependence in **1** is larger than that of **2**, although both correlations are excellent ($r > 0.999$). The results show that **2** (**B**: **pd**) are thermally very stable and other conformers are substantially negligible in the solution for all Y examined. **1** (**A**: **pl**) must also be predominant in solutions, although **1** (**A**: **pl**) would not be thermally so stable, relative to the case of **2** (**B**: **pd**).

[1] The contribution of relativistic terms has been pointed out for heavier atoms, but the perturbation would be small for the selenium nucleus.

[2] This decomposition includes small arbitrariness due to the coordinate origin dependence, though it does not damage our chemical analyses and insights into the ^{77}Se NMR spectroscopy.

[3] The 0.050 M $CDCl_3$ solutions were used for NMR measurements. However, the concentrations would be lower for the compounds of low solubility, such as **1j** and **2j**, especially at 213 K.

Table 1: Observed $\delta(\mathrm{Se})_{\mathrm{SCS}}$ of **1** and **2** and calculated $\sigma^t_{\mathrm{rel}}(\mathrm{Se})_{\mathrm{SCS}}$ for **4–6** in **pl** and **pd**[a,b].

Compd	T [K]	NMe_2 (**b**)	OMe (**c**)	Me (**d**)	H (**a**)	F (**e**)	Cl (**f**)	Br (**g**)	CO_2R[c] (**h**)	CN (**i**)	NO_2 (**j**)
1	213	−22.7	−12.7	−6.3	0.0 (245.3)	−3.3	1.9	2.4	17.4	27.7	32.7
1	297	−21.0	−12.2	−6.6	0.0 (249.0)	−3.6	1.5	1.6	16.2	26.2	30.4
1	333	−21.3	−12.7	−6.8	0.0 (250.6)	−3.9	1.0	1.2	15.2	24.8	29.0
2	213	−20.6	−15.5	−9.2	0.0 (511.4)	−10.5	−7.1	−6.4	0.1	8.5	2.7
2	297	−19.6	−15.0	−9.0	0.0 (512.3)	−10.2	−7.1	−6.4	0.0	8.2	2.5
2	333	−19.5	−15.0	−9.1	0.0 (512.5)	−10.3	−7.2	−6.7	−0.3	7.9	2.2
4 (**pl**)	—	−36.4	−18.0	−8.2	0.0 (87.0)	−1.6	1.7	−1.8	14.3	29.8	33.7
4 (**pd**)	—	−35.9	−23.0	−15.6	0.0 (41.3)	−11.8	−9.1	−8.7	1.0	16.8	10.0
5 (**pl**)	—	−23.9	−8.2	−8.0	0.0 (169.7)	2.1	4.7	7.2	24.6	29.7	43.8
5 (**pd**)	—	−34.9	−21.2	−16.7	0.0 (219.1)	−14.1	−11.8	−12.6	3.0	13.4	6.6
6 (**pl**)	—	−20.5	−9.0	−3.7	0.0 (398.8)	1.1	1.9	2.3	13.1	20.2	28.6
6 (**pd**)	—	−34.2	−25.8	−14.6	0.0 (398.8)	−15.2	−13.3	−12.6	−3.4	7.0	0.5

[a] $\delta(\mathrm{Se})_{\mathrm{SCS}}$ are given for **1** and **2**, together with δ(Se) for **1** a and **2** a in parenthesis, measured in chloroform-*d*.
[b] $\sigma^t_{\mathrm{rel}}(\mathrm{Se})_{\mathrm{SCS}}$ are given for **4–6**, together with σ^t_{rel}(Se) for **4a–6a** in parenthesis, calculated according to (3), where σ^t(Se) of **4–6** in **pl** and **pd** are given in Tables 3–5, respectively, and σ^t(Se: MeSeMe) = 1650.4 ppm.
[c] R = Et for **1** and **2** and R = Me for **4–6**.

Table 2: Correlations of $\delta(\mathrm{Se})_{\mathrm{SCS}}$ for **1** and **2** and σ(Se) for **4–6**, together with $\delta(\mathrm{Se})_{\mathrm{SCS}}$ for **5–9**[a].

Entry	Correlation	a	b	r	n[b]
1	δ(Se: **1**)$_{\mathrm{SCS,\ 297\,K}}$ vs δ(Se: **1**)$_{\mathrm{SCS,\ 213\,K}}$	0.940	−0.3	1.000	10
2	δ(Se: **1**)$_{\mathrm{SCS,\ 333\,K}}$ vs δ(Se: **1**)$_{\mathrm{SCS,\ 213\,K}}$	0.916	−0.8	1.000	10
3	δ(Se: **2**)$_{\mathrm{SCS,\ 297\,K}}$ vs δ(Se: **2**)$_{\mathrm{SCS,\ 213\,K}}$	0.957	−0.1	1.000	10
4	δ(Se: **2**)$_{\mathrm{SCS,\ 333\,K}}$ vs δ(Se: **2**)$_{\mathrm{SCS,\ 213\,K}}$	0.946	−0.3	1.000	10
5	δ(Se: **1**)$_{\mathrm{SCS,\ 213\,K}}$ vs σ^{rel}(Se: **4** (**pl**))$_{\mathrm{SCS}}$	0.823	2.6	0.986	10
6	δ(Se: **1**)$_{\mathrm{SCS,\ 213\,K}}$ vs σ^{rel}(Se: **5** (**pl**))$_{\mathrm{SCS}}$	0.845	−2.1	0.990	10
7	δ(Se: **1**)$_{\mathrm{SCS,\ 213\,K}}$ vs σ^{rel}(Se: **6** (**pl**))$_{\mathrm{SCS}}$	1.218	−0.4	0.991	10
8	δ(Se: **2**)$_{\mathrm{SCS,\ 213\,K}}$ vs σ^{rel}(Se: **4** (**pd**))$_{\mathrm{SCS}}$	0.562	−1.5	0.990	10
9	δ(Se: **2**)$_{\mathrm{SCS,\ 213\,K}}$ vs σ^{rel}(Se: **5** (**pd**))$_{\mathrm{SCS}}$	0.599	−0.5	0.988	10
10	δ(Se: **2**)$_{\mathrm{SCS,\ 213\,K}}$ vs σ^{rel}(Se: **6** (**pd**))$_{\mathrm{SCS}}$	0.691	1.9	0.990	10
11	σ^p(Se) vs $(\sigma^p(\mathrm{Se})_{xx} + \sigma^p(\mathrm{Se})_{yy})$ in **4** (**pl**)	0.339	−547.8	0.982	10
12	σ^p(Se) vs $(\sigma^p(\mathrm{Se})_{xx} + \sigma^p(\mathrm{Se})_{yy})$ in **5** (**pl**)	0.367	−461.8	0.999	10
13	σ^p(Se) vs $(\sigma^p(\mathrm{Se})_{xx} + \sigma^p(\mathrm{Se})_{yy})$ in **6** (**pl**)	0.350	−546.7	0.990	10
14	σ^p(Se) vs $(\sigma^p(\mathrm{Se})_{xx} + \sigma^p(\mathrm{Se})_{yy})$ in **4** (**pd**)	0.309	−547.0	0.998	10
15	σ^p(Se) vs $(\sigma^p(\mathrm{Se})_{xx} + \sigma^p(\mathrm{Se})_{yy})$ in **5** (**pd**)	0.345	−517.4	0.994	10
16	σ^p(Se) vs $(\sigma^p(\mathrm{Se})_{xx} + \sigma^p(\mathrm{Se})_{yy})$ in **6** (**pd**)	0.335	−598.5	0.998	10
17	δ(Se: **5**)$_{\mathrm{SCS}}$[c] vs δ(Se: **1**)$_{\mathrm{SCS,\ 213\,K}}$	0.997	1.0	0.997	8
18	δ(Se: **5**)$_{\mathrm{SCS}}$[d] vs δ(Se: **1**)$_{\mathrm{SCS,\ 213\,K}}$	0.952	0.1	0.999	7
19	δ(Se: **7**)$_{\mathrm{SCS}}$ vs δ(Se: **2**)$_{\mathrm{SCS,\ 213\,K}}$	0.909	1.3	0.995	10
20	δ(Se: **6**)$_{\mathrm{SCS}}$ vs δ(Se: **1**)$_{\mathrm{SCS,\ 213\,K}}$	0.804	−3.3	0.991	7
21	δ(Se: **8**)$_{\mathrm{SCS}}$ vs δ(Se: **1**)$_{\mathrm{SCS,\ 213\,K}}$	0.691	−1.7	0.981	9
22	δ(Se: **9**)$^{\mathrm{c}}_{\mathrm{SCS}}$ vs δ(Se: **1**)$_{\mathrm{SCS,\ 213\,K}}$	0.870	−1.3	0.999	7

[a] The constants (a, b, r) are defined by $y = ax + b$ (r: correlation coefficient).
[b] The number of data used in the correlation. [c] Reference [19] at neat. [d] Reference [11] in $CDCl_3$.

Scheme 2 shows the axes and some orbitals of **4–6**, together with SeH_2. While the x-axis of SeH_2 is in the bisected direction of ∠HSeH, the Se−H and Se−C bonds of MeSeH are almost on the x- and y-axes, respectively, although not

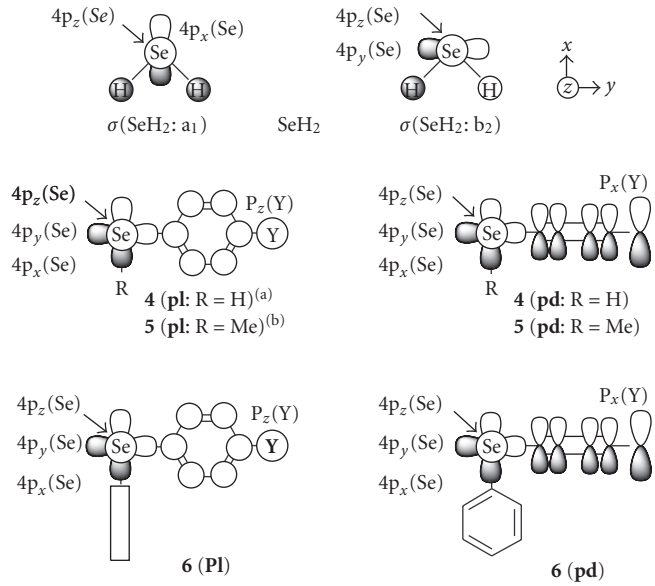

[a] Axes with Y = Br and COOMe are close to those for SeH_2

[b] Axes with Y = Me and CN are close to those for SeH_2

Scheme 2: Axes and some orbitals of **4–6**, together with those of SeH_2.

shown. Axes of **4–6** are close to those in MeSeH in most cases. Since ∠CSeX (X = H or C) in **4–6** are about 95°, 98°, and 101°, respectively, the Se−C and Se−H bonds deviate inevitably from the axes to some extent. Axes are rather similar to those of SeH_2 for **4** (**pl**) with Y = Br and COOMe and **5** (**pl**) with Y = Me and CN.[4]

Structures of **4–6** in **pl** and **pd** are optimized employing the 6-311+G(3df) basis sets for Se and the 6-311+G(3d,2p) basis sets for other nuclei of the Gaussian 03 program [47].[5] Calculations are performed at the density functional theory (DFT) level of the Becke three parameter hybrid functionals with the Lee-Yang-Parr correlation functional (B3LYP). Absolute magnetic shielding tensors of Se (σ(Se)) are calculated based on the DFT-GIAO method [42–46], applying on the optimized structures with the method. Tables 3–5 collect σ^t(Se), σ^d(Se), σ^p(Se), and the components of σ^p(Se), $\sigma^p(\mathrm{Se})_{xx}$, $\sigma^p(\mathrm{Se})_{yy}$, and $\sigma^p(\mathrm{Se})_{zz}$ for **4–6** bearing various substituents Y in **pl** and **pd**, respectively.[6]

Relative shielding constants of **A** (σ^t_{rel}(Se: **A**)) are calculated for **4–6** according to (3), using σ^t(Se: MeSeMe) (= 1650.4 ppm). $\sigma^t_{\mathrm{rel}}(\mathrm{Se{:}\ A})_{\mathrm{SCS}}$ are calculated similarly. Table 1 also contains σ^t_{rel}(Se: **A**) of **4a–6a** and $\sigma^t_{\mathrm{rel}}(\mathrm{Se{:}\ A})_{\mathrm{SCS}}$ for **4–6**,

$$\sigma^t_{\mathrm{rel}}(\mathrm{Se:A}) = -\{\sigma^t(\mathrm{Se:A}) - \sigma^t(\mathrm{Se:MeSeMe})\} \quad (\mathbf{A}:\mathbf{n}(\mathbf{pl}),\mathbf{n}(\mathbf{pd})). \tag{3}$$

Table 6 shows $\sigma(\mathrm{Se})_{\mathrm{SCS}}$ of *p*-$YC_6H_4SeCOPh$ (**7**) [13], *p*-YC_6H_4SeCN (**8**) [8], and bis[8-(arylselanyl)naphthyl] 1,1′-diselenides (**9**) [15, 16], together with **5** [11, 19] and **6** [15, 16] (see Chart 2). The values are plotted versus $\delta(\mathrm{Se{:}\ 1})_{\mathrm{SCS}}$ and/or $\delta(\mathrm{Se{:}\ 2})_{\mathrm{SCS}}$ to explain the δ(Se) based on the orientational effect of the aryl groups.

DISCUSSION

Characters in δ(Se: 1) and δ(Se: 2)

The structures of all members of **1** and **2** are confirmed to be **1** (**A**: **pl**) and (**B**: **pd**), respectively, (see Scheme 1) [25]. The nature of δ(Se: **1**) must be the results of **1** (**A**: **pl**), where n_p(Se) is parallel to the $\pi(C_6H_4Y\text{-}p)$. Characteristic points in $\delta(\mathrm{Se{:}\ 1})_{\mathrm{SCS}}$ are summarized as follows.

(1) Large upfield shifts (−23 ppm to −6 ppm) are observed for Y = NMe_2, OMe, and Me and large downfield shifts (17 ppm to 33 ppm) are for Y = COOEt, CN, and NO_2, relative to Y = H.

(2) Moderate upfield shift (−3 ppm) is observed for Y = F.

[4] When the axes from the Gaussian 03 program [47] are not the same as those shown in Scheme 3, axes are interchanged so as to be those in Scheme 3 for convenience of discussion, if possible.

[5] Gaussian 03 (Revision B.05).

[6] The torsional angle of $\phi = C_oC_iSeH$ in **4** (**pd**) is fixed at 90.0° if **4** (**pd**) is not the *Cs* symmetry (eg, Y = COOMe and OMe). Similarly, those of $\phi = C_oC_iSeC_{Me}$ and $\phi = C_iSeC_{Me}H$ in **5** (**pd**) are fixed at 90.0° and 180°, respectively, and those of $\phi = C_oC_iSeC_{i'}$ and $\phi = C_iSeC_{i'}C_{o'}$ in **6** (**pd**) are fixed at 90.0° and 0°, respectively, when the conformers are not the *Cs* symmetry.

(3) Small downfield shifts (2 ppm) are for Y = Cl and Br: the three points corresponding to Y = H, Cl, and Br are found very close with each other.

The characters of δ(Se: **2**)$_{SCS}$ are very different from those of δ(Se: **1**)$_{SCS}$. The characteristics must be the reflection of **2** (**B**: **pd**), where n_p(Se) is perpendicular to $\pi(C_6H_4Y\text{-}p)$. Characteristic points of δ(Se: **2**)$_{SCS}$ are as follows.

(1) Large upfield shifts (−21 to −6 ppm) are observed for Y = NMe_2, OMe, Me, F, Cl, and Br, relative to Y = H.
(2) Downfield shifts (3 ppm to 9 ppm) are brought by Y = CN and NO_2, where the magnitude by Y = CN is larger than that by NO_2.
(3) δ(Se: **2**)$_{SCS}$ brought by Y = COOEt is negligible.

While δ(Se: **1**)$_{SCS}$ is in a range of $-23 < \delta(Se)_{SCS} < 33$ ppm, δ(Se: **2**)$_{SCS}$ is $-21 < \delta(Se)_{SCS} < 9$ ppm. Y of both donors and acceptors operate well on δ(Se: **1**)$_{SCS}$, whereas only Y of donors do well on δ(Se: **2**)$_{SCS}$.

δ(Se: **2**)$_{SCS}$ are plotted versus those of δ(Se: **1**)$_{SCS}$. Figure 1 shows the results. Indeed, it emphasizes the difference in the characters between δ(Se: **1**)$_{SCS}$ and δ(Se: **2**)$_{SCS}$, but most of δ(Se: **2**)$_{SCS}$ seem to correlate well with δ(Se: **1**)$_{SCS}$, as shown by a dotted line ($a = 0.58$). Two points corresponding to Y = H and NO_2 deviate upside and downside from the line, respectively. Namely, points for **2** with Y of non-H are more downside (upfield) than expected from δ(Se: **1a**)$_{SCS}$ and δ(Se: **2a**)$_{SCS}$, especially for δ(Se: **2j**)$_{SCS}$.

Why are such peculiar behaviors observed in **1** and **2**, caused by the orientational effect of the aryl group? The mechanism is elucidated based on the QC calculations performed on **4**–**6**, assuming **pl** and **pd** for each.

Observed δ(Se) versus calculated σ^t(Se)

The $\delta(Se)_{SCS}$ values of **1** and **2** are plotted versus $\sigma^t_{rel}(Se)_{SCS}$ of **4** (**pl**)–**6** (**pl**) and **4** (**pd**)–**6** (**pd**), respectively, (Table 1). Good correlations are obtained as shown in Table 2 (entries 5–10). The r values become larger in an order of **4**(**pl**) < **5**(**pl**) $\leqq$ **6**(**pl**) for **1** and in an order of **5**(**pd**) < **4**(**pd**) $\approx$ **6**(**pd**) for **2**. Namely, observed δ(Se: **1**)$_{SCS}$ and δ(Se: **2**)$_{SCS}$ are reproduced by σ^t_{rel}(Se: **6** (**pl**))$_{SCS}$ and σ^t_{rel}(Se: **6** (**pd**))$_{SCS}$, respectively, in most successfully. Figure 2 exhibits the plots for (a) **1** versus **6** (**pl**) and (b) **2** versus **6** (**pd**). The correlations are given in Table 2 (entries 7 and 10). The results demonstrate that the characters of $\delta(Se)_{SCS}$ observed in **1** originate from the planar structure and those in **2** from the characteristic structure, where Se−C_{Atq} in p-YC_6H_4SeAtq is perpendicular to the p-YC_6H_4 plane.

How does such orientational effect arise from the structures? How does the electronic property of Y affect on δ(Se) of **1** and **2**? σ^p(Se) of **4**–**6** are analyzed next.

Orientational effect in 4a–6a

σ(Se) of **4**–**6** shown in Tables 3–5 are examined. σ^p(Se) and σ^t(Se) of **4a** (**pd**) are evaluated to be larger (more upfield) than those of **4a** (**pl**) by 43 ppm and 46 ppm, respectively,

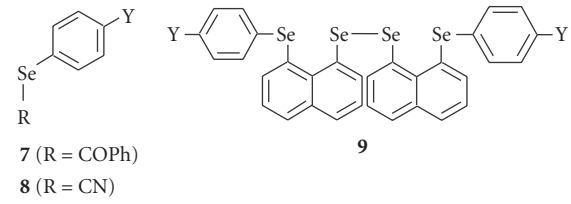

7 (R = COPh)
8 (R = CN)
9

Chart 2

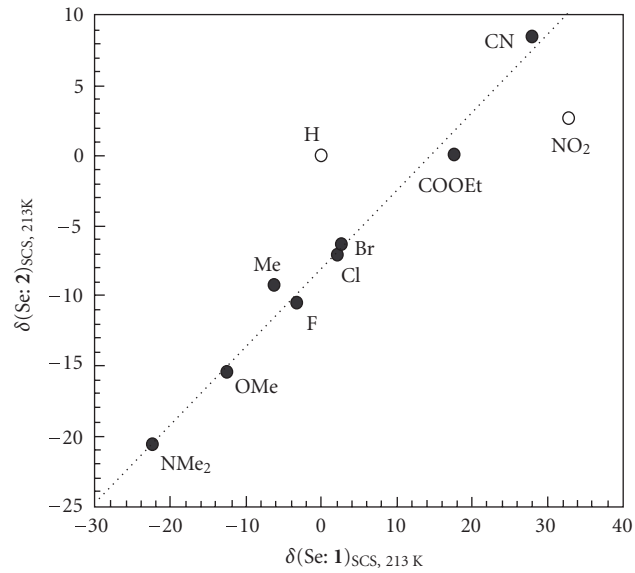

Figure 1: Plot of δ(Se: **2**)$_{SCS,\ 213\,K}$ versus δ(Se: **1**)$_{SCS,\ 213\,K}$.

which correspond to the orientational effect caused by Ph in **4a**.[7] The inverse orientational effect is predicted for **5a**. σ^p(Se) and σ^t(Se) of **5a** (**pd**) are smaller than those of **5a** (**pl**) by 41 ppm and 49 ppm, respectively. While σ^p(Se) and σ^t(Se) of **5a** (**pl**) are smaller than those of **4a** (**pl**) by 90 ppm and 83 ppm, respectively, the values of **5a** (**pd**) are smaller than those of **4a** (**pd**) by 174 ppm and 178 ppm, respectively. The differences are −84 ppm and −95 ppm, respectively, which also correspond to the differences in the orientational effect of the Ph group between **5a** and **4a**, respectively. The more effective contribution to downfield shifts by the Se−C_{Me} bond in **5a** (**pd**), relative to **5a** (**pl**), must be responsible for the results. The orientational effect cannot be discussed for **6a** of the *Cs* symmetry with Y = H.

[7] The DFT shieldings are deshielded in general, due to the underestimation of the orbital energy differences, which lead to the overestimation of the σ^p(Se) [48]. MP2 calculations are also performed on **4a** (**pl**), **4a** (**pd**), **5a** (**pl**), and **5a** (**pd**). The geometries are optimized with the MP2/6-311+G(3d,2p) method. σ^t(Se) are calculated with the MP2-GIAO method, employing the 6-311+G(2d,p) basis sets. The results are as follows (in ppm): (σ^t(Se: **4a** (**pl**)), σ^t(Se: **4a** (**pd**))) = (1827.3, 1865.5) and (σ^t(Se: **5a** (**pl**)), σ^t(Se: **5a** (**pd**))) = (1761.0, 1708.7). σ^t(Se: **4a** (**pl**)) is evaluated to be more downfield than σ^t(Se: **4a** (**pd**)) by 38 ppm, whereas σ^t(Se: **5a** (**pl**)) is evaluated to be more upfield than σ^t(Se: **5a** (**pd**)) by 52 ppm. The results support the orientational effects evaluated at the DFT level for **4a** and **5a**, although the basis sets are not the same.

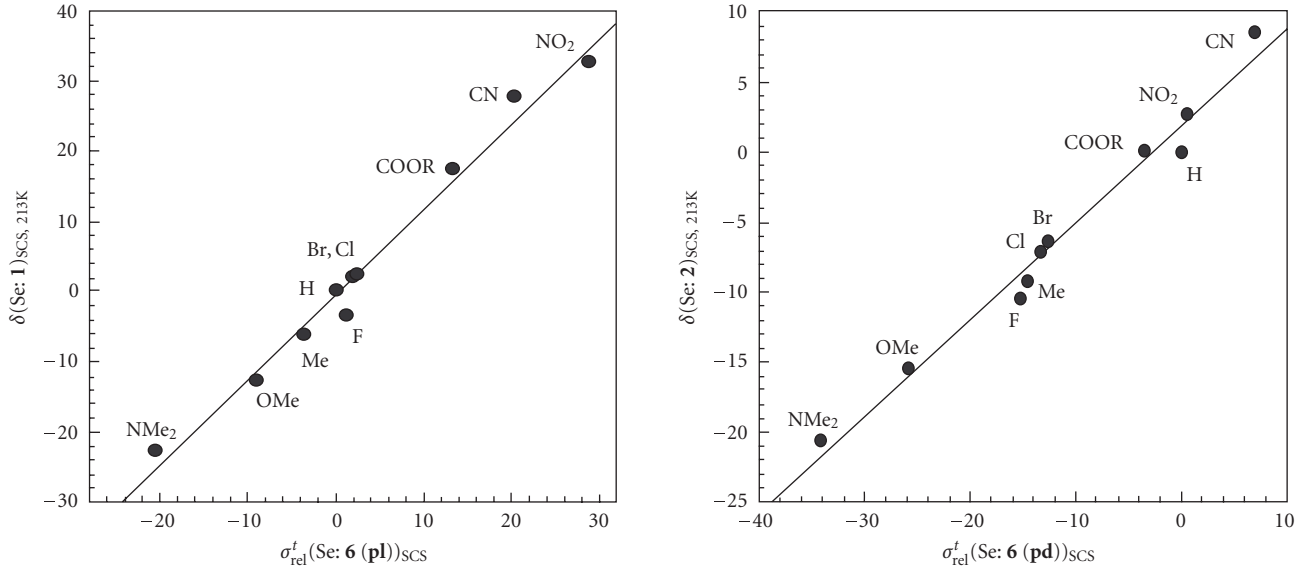

FIGURE 2: Plots of (a) δ(Se: **1**)$_{SCS,\ 213\,K}$ versus σ^t_{rel}(Se: **6** (**pl**))$_{SCS}$ and (b) δ(Se: **2**)$_{SCS,\ 213\,K}$ versus σ^t_{rel}(Se: **6** (**pd**))$_{SCS}$.

What mechanism is operating in the Y dependence? σ^p(Se) of **4–6** in **pl** and **pd** are analyzed next.

Y dependence in 4–6

To get an image in the behavior of $\sigma^p(\mathrm{Se})_{xx}$, $\sigma^p(\mathrm{Se})_{yy}$, and $\sigma^p(\mathrm{Se})_{zz}$ of **4–6**, the values are plotted versus σ^p(Se). Figure 3 shows the plots for **4** (**pd**) and **6** (**pl**). The correlations in **4** (**pd**) are linear and both $\sigma^p(\mathrm{Se})_{xx}$ and $\sigma^p(\mathrm{Se})_{yy}$ increase along with σ^p(Se). The plot for **5** (**pd**) is similar to that for **4** (**pd**), although not shown. In the case of **6** (**pl**), the correlations are linear but the slope for $\sigma^p(\mathrm{Se})_{yy}$ is inverse to that for $\sigma^p(\mathrm{Se})_{xx}$. The plots of $\sigma^p(\mathrm{Se})_{xx}$ and $\sigma^p(\mathrm{Se})_{yy}$ do not give smooth lines for **4** (**pl**), **5** (**pl**), and **6** (**pd**). However, the slopes for $\sigma^p(\mathrm{Se})_{zz}$ are very smooth and the magnitudes are very close to 1.0 for all cases in **4–6**.

To clarify the behavior of σ^p(Se) in **4–6**, σ^p(Se) are plotted versus $(\sigma^p(\mathrm{Se})_{xx} + \sigma^p(\mathrm{Se})_{yy})$.[8] Excellent to good correlations are obtained in all cases as collected in Table 2 (entries 11–16). Figure 4 exhibits the plot of σ^p(Se) for **6** (**pd**), for example. The correlation constants (a) are 0.31–0.37, which are very close to one third. The results exhibit that $(\sigma^p(\mathrm{Se})_{xx}+\sigma^p(\mathrm{Se})_{yy})$ determines σ^p(Se) of **4–6** effectively (cf: (2)). The observations led us to establish the mechanism of Y dependence in **4–6**.

Mechanism of Y dependence

The mechanism of Y dependence in **4–6** is elucidated by exemplifying **4**. As shown in Scheme 2, the main interaction between Se and Y in **4** (**pl**) is the 4p$_z$(Se)-π(C$_6$H$_4$)-p$_z$(Y) type, which modifies the contributions of 4p$_z$(Se) in π(SeC$_6$H$_4$Y) and π^*(SeC$_6$H$_4$Y). Since $(\sigma^p(\mathrm{Se})_{xx} + \sigma^p(\mathrm{Se})_{yy})$ controls σ^p(Se) of **4** (**pl**) effectively, admixtures between 4p$_z$(Se) in modified π(SeC$_6$H$_4$Y) and π^*(SeC$_6$H$_4$Y) with 4p$_y$(Se) and 4p$_x$(Se) in σ(C$_{Ar}$SeH) and σ^*(C$_{Ar}$SeH) must originate the Y dependence mainly when a magnetic field is applied.[9] Since $\sigma^p_{zz,N}$ contains the $\hat{L}_{z,N}$ operator, $\sigma^p_{zz,N}$ arises from admixtures between atomic p$_x$ and p$_y$ orbitals of N in various molecular orbitals. When a magnetic field is applied on a selenium compound, mixings of unoccupied molecular orbitals (MO's; ψ_i) into occupied orbital MO's (ψ_i) will occur. Such admixtures generate $\sigma^p_{zz,N}$ if ψ_i and ψ_j contain p$_x$ and p$_y$ of N, for example. $\sigma^p_{xx,N}$ and $\sigma^p_{yy,N}$ are also understood similarly. Consequently, Y of both donors and acceptors are effective for the Y dependence in **4** (**pl**). Scheme 3(a) shows the mechanism for **pl**.

In the case of **4** (**pd**), 4p$_z$(Se) remains in n$_p$(Se) in the almost pure form.[10] The σ(C$_{Ar}$SeH)-π(C$_6$H$_4$)-p$_x$(Y) interaction occurs instead, which modifies the contributions of 4p$_x$(Se) and 4p$_y$(Se) in σ(C$_{Ar}$SeH) and σ^*(C$_{Ar}$SeH)

[8] $\sigma^p(\mathrm{Se})_{zz}$ is almost constant in the change of Y for both **pl** and **pd** in **4–6**. The small Y-dependence of $\sigma^p(\mathrm{Se})_{zz}$ is reasonably explained through the main interaction of the 4p$_z$(Se)-π(C$_6$H$_4$)-p$_z$(Y) type in **pl**, where 4p$_x$(Se) and 4p$_y$(Se) do not take part in the interaction directly. The main interaction in **pd** is the σ(C$_{Ar}$SeX)-π(C$_6$H$_4$)-p$_x$(Y) (X = H or C) type, which modifies the contributions of 4p$_x$(Se) and 4p$_y$(Se) in the C$_{Ar}$SeX bonds. However, the results show that the interaction in **pd** affects on $\sigma^p(\mathrm{Se})_{xx}$ and $\sigma^p(\mathrm{Se})_{yy}$ but not on $\sigma^p(\mathrm{Se})_{zz}$.

[9] σ^p is exactly expressed by Ramsey's equation [49]. While σ^p is evaluated accurately by the CPHF method, it is approximated as $\sigma^p_{zz,N} = -(\mu_o e^2/2m_e^2)\Sigma_i^{occ}\Sigma_j^{unocc}(\varepsilon_j - \varepsilon_i)^{-1} \times \{< \psi_i|\hat{L}_z|\psi_j >< \psi_j|\hat{L}_{z,N}r_N^{-3}|\psi_i > + < \psi_i|\hat{L}_{z,N}r_N^{-3}|\psi_j >< \psi_j|\hat{L}_z|\psi_i >\}$.

[10] The interactions between n$_p$(Se) of 4p$_z$(Se) and phenyl σ orbitals in **4a** (**pd**) must be weak due to large energy differences between 4p$_z$(Se) and the σ orbitals. Long distances between them are also disadvantageous.

Table 3: Calculated absolute shielding tensors (σ(Se)) of **4**, containing various Y[(a)].

Y	σ^d(Se)	$\sigma^p(\mathrm{Se})_{xx}$	$\sigma^p(\mathrm{Se})_{yy}$	$\sigma^p(\mathrm{Se})_{zz}$	σ^p(Se)	σ^t(Se)
			4 (**pl**)			
H	2999.5	−1571.7	−1042.3	−1694.2	−1436.1	1563.4
NMe_2	3006.4	−1676.1	−862.4	−1681.4	−1406.7	1599.8
OMe	3004.7	−1823.5	−757.0	−1689.5	−1423.3	1581.4
Me	3002.4	−1760.2	−848.1	−1684.2	−1430.8	1571.6
F	3001.4	−1800.4	−833.2	−1675.7	−1436.4	1565.0
Cl	3003.8	−1777.8	−868.7	−1680.0	−1442.2	1561.7
Br	3008.7	−1883.4	−745.3	−1701.6	−1443.4	1565.2
COOMe	3010.0	−1469.6	−1197.4	−1715.7	−1460.9	1549.1
CN	3002.1	−1829.1	−889.8	−1686.5	−1468.5	1533.6
NO_2	3004.9	−1836.6	−905.8	−1683.2	−1475.2	1529.7
			4 (**pd**)			
H	3001.9	−1870.9	−869.9	−1437.6	−1392.8	1609.1
NMe_2	3004.1	−1782.2	−842.4	−1452.8	−1359.1	1645.0
OMe	3005.4	−1805.2	−871.3	−1443.6	−1373.4	1632.1
Me	3002.2	−1821.7	−871.0	−1439.8	−1377.5	1624.7
F	3000.8	−1829.8	−866.2	−1443.7	−1379.9	1620.9
Cl	3000.8	−1834.5	−870.2	−1442.8	−1382.5	1618.2
Br	3000.5	−1835.5	−870.5	−1442.1	−1382.7	1617.8
COOMe	3004.2	−1872.6	−879.2	−1436.5	−1396.1	1608.1
CN	2999.9	−1901.0	−881.6	−1440.1	−1407.6	1592.3
NO_2	3000.7	−1877.7	−884.4	−1442.8	−1401.6	1599.1

[(a)] Structures are optimized with the 6-311+G(3df) basis sets for Se and 6-311+G(3d,2p) basis sets for other nuclei at the DFT (B3LYP) level, assuming **pl** and **pd** for each of Y [47]. σ(Se) are calculated based on the DFT-GIAO method with the same methods.

(see Scheme 2). $(\sigma^p(\mathrm{Se})_{xx} + \sigma^p(\mathrm{Se})_{yy})$ determines effectively σ^p(Se) of **4** (**pd**). Therefore, Y dependence of **4** (**pd**) originates mainly from admixtures between $4p_z$(Se) in n_p(Se) and $4p_x$(Se) and $4p_y$(Se) in modified $\sigma^*(C_{Ar}SeH)$ since n_p(Se) of $4p_z$(Se) is filled with electrons. Consequently, Y dependence in **4** (**pd**) must be more sensitive to Y of donors, which is a striking contrast to the case of **4** (**pl**). Scheme 3(b) summarizes the mechanism for **pd**.

The mechanisms proposed for **4** (**pl**) and **4** (**pd**) must be applicable to **5** and **6**. The expectations are just observed in δ(Se: **1**)$_{SCS}$ and δ(Se: **2**)$_{SCS}$.

Applications of δ(Se: 1) and δ(Se: 2) as the standards

Odom made a lot of effort to explain δ(Se) of **7** based on the electronic effect of Y [13]. However, the attempt was not successful: δ(Se: **7**) were not correlated well with δ(Se: **5**). How are δ(Se) of p-YC_6H_4SeR interpreted based on the orientational effect? Our explanation for the relationship between δ(Se) of p-YC_6H_4SeR and the structures is as follows.

Figure 5 shows the plot of δ(Se: **5**)$_{SCS}$ measured in $CDCl_3$ [19] versus δ(Se: **1**)$_{SCS,\ 213\,K}$ and the correlation is given in Table 2 (entry 17: $r = 0.997$). The correlation coefficient is excellent when δ(Se: **5**)$_{SCS}$ measured in neat is plotted versus δ(Se: **1**)$_{SCS,\ 213\,K}$ (entry 18 in Table 2: $r = 0.999$). These observations must be the results of the Se−C_{Me} bond in **5** being on the p-YC_6H_4 plane in solutions for all Y examined, under the conditions. On the other hand, δ(Se: **7**)$_{SCS}$ do not correlate with δ(Se: **1**)$_{SCS,\ 213\,K}$. Instead, they correlate well with δ(Se: **2**)$_{SCS,\ 213\,K}$ (entry 19 in Table 2: $r = 0.995$). Figure 6 shows the plot. The results are rationally explained by assuming that the Se−C_O bond in **7** is perpendicular to the p-YC_6H_4 plane in solutions for all Y examined, under the conditions.

$\delta(\mathrm{Se})_{SCS}$ of **6** [19] and **8** [8] are similarly plotted versus δ(Se: **1**)$_{SCS,\ 213\,K}$. They give good correlations, although the r values become poorer relative to that for **5** (entries 20 and 21

Table 4: Calculated absolute shielding tensors (σ(Se)) of **5**, containing various Y[(a)].

Y	σ^d(Se)	$\sigma^p(\mathrm{Se})_{xx}$	$\sigma^p(\mathrm{Se})_{yy}$	$\sigma^p(\mathrm{Se})_{zz}$	σ^p(Se)	σ^t(Se)
			5 (**pl**)			
H	3006.5	−1893.4	−999.0	−1684.9	−1525.8	1480.7
NMe_2	3007.7	−1645.4	−1194.5	−1669.5	−1503.1	1504.6
OMe	3007.4	−1741.5	−1136.8	−1677.1	−1518.4	1488.9
Me	3008.0	−1815.2	−1064.7	−1678.0	−1519.3	1488.7
F	3006.2	−1911.7	−990.8	−1680.6	−1527.7	1478.6
Cl	3006.7	−1639.8	−1269.8	−1682.4	−1530.7	1476.0
Br	3008.1	−1768.8	−1156.2	−1679.0	−1534.7	1473.5
COOMe	3009.6	−1840.5	−1132.8	−1687.1	−1553.5	1456.1
CN	3006.6	−1601.6	−1377.0	−1688.1	−1555.6	1451.0
NO_2	3007.0	−1800.0	−1220.1	−1690.0	−1570.1	1436.9
			5 (**pd**)			
H	2998.0	−1956.8	−1086.4	−1656.9	−1566.7	1431.3
NMe_2	3003.5	−1889.2	−1062.0	−1660.9	−1537.3	1466.2
OMe	3004.1	−1938.6	−1059.6	−1656.6	−1551.6	1452.5
Me	2999.8	−1908.0	−1090.1	−1657.2	−1551.8	1448.0
F	2998.1	−1916.6	−1077.7	−1663.9	−1552.8	1445.4
Cl	2999.3	−1925.8	−1078.6	−1664.3	−1556.2	1443.1
Br	3001.0	−1930.0	−1077.7	−1663.5	−1557.1	1443.9
COOMe	3006.4	−2017.8	−1057.8	−1658.7	−1578.1	1428.3
CN	2998.0	−1995.5	−1076.6	−1668.2	−1580.1	1417.9
NO_2	2999.5	−1977.4	−1075.9	−1671.0	−1574.7	1424.7

[(a)]Structures are optimized with the 6-311+G(3df) basis sets for Se and 6-311+G(3d,2p) basis sets for other nuclei at the DFT (B3LYP) level, assuming **pl** and **pd** for each of Y [47]. σ(Se) are calculated based on the DFT-GIAO method with the same methods.

in Table 2). The reason would be the equilibrium of **pl** with **pd** for some Y in **6** and **8**, may be Y of donors.

$\delta(\mathrm{Se})_{\mathrm{SCS}}$ of **9** are also plotted versus $\delta(\mathrm{Se}: \mathbf{1})_{\mathrm{SCS,\ 213\,K}}$. The correlations are excellent (entry 22 in Table 2: $r = 0.999$). It is worthwhile to comment that the energy lowering effect by Se_4 4c–6e in **9** fixes the conformation **9** (**pl**, **pl**) for both *p*-YC_6H_4Se groups in solutions for all Y examined, under the conditions [50].

It is demonstrated that sets of δ(Se: **1**) and δ(Se: **2**) proposed in this work can be the standards for **pl** and **pd**, respectively, when δ(Se) of aryl selenides are analyzed based on the orientational effect.

CONCLUSION

The orientational effect is empirically established by the Y dependence on δ(Se: **1**) and δ(Se: **2**). The Y dependence observed in **1** and **2** is demonstrated by σ^t(Se) calculated for **4**–**6** with the DFT-GIAO method. While σ^t(Se) of **4a** (**pl**) is predicted to be more negative than that of **4a** (**pd**) by 46 ppm, σ^t(Se) of **5a** (**pl**) is evaluated to be larger than that of **5a** (**pd**) by 49 ppm, which corresponds to the orientational effect by the Ph group in **4a** and **5a**, respectively. Excellent to good correlations are obtained in the plots of σ^p(Se) versus $(\sigma^p(\mathrm{Se})_{xx} + \sigma^p(\mathrm{Se})_{yy})$ for **4**–**6** in **pl** and **pd**. It is demonstrated that $(\sigma^p(\mathrm{Se})_{xx} + \sigma^p(\mathrm{Se})_{yy})$ effectively controls σ^p(Se) of **4**–**6** in **pl** and **pd**.

The mechanisms of the Y dependence are proposed based on the magnetic perturbation theory. The main interaction in **pl** is the n_p(Se)-$\pi(C_6H_4)$-p_z(Y) conjugation. Y dependence in **pl** occurs through admixtures of $4p_z$(Se) in modified $\pi(SeC_6H_4Y)$ and $\pi^*(SeC_6H_4Y)$ with $4p_x$(Se) and $4p_y$(Se) in σ(CSeX) and σ^*(CSeX) (X = H or C). The main interaction in **pd** is the σ(CSeX)-$\pi(C_6H_4)$-p_x(Y) type, which modifies both $\sigma(C_{Ar}SeH)$ and $\sigma^*(C_{Ar}SeH)$. The Y dependence in **pd** mainly originates from admixtures

Table 5: Calculated absolute shielding tensors (σ(Se)) of **6**, containing various Y[(a)].

Y	σ^d(Se)	$\sigma^p(\mathrm{Se})_{xx}$	$\sigma^p(\mathrm{Se})_{yy}$	$\sigma^p(\mathrm{Se})_{zz}$	σ^p(Se)	σ^t(Se)
			6 (**pl**)			
H	2995.1	−1527.4	−1887.5	−1815.6	−1743.5	1251.6
NMe_2	2997.7	−1462.8	−1902.3	−1811.6	−1725.5	1272.1
OMe	2995.5	−1504.1	−1887.4	−1813.2	−1734.9	1260.6
Me	2995.6	−1517.7	−1888.8	−1814.2	−1740.3	1255.3
F	2994.5	−1544.4	−1879.4	−1808.1	−1743.9	1250.5
Cl	2994.1	−1550.2	−1873.8	−1809.2	−1744.4	1249.7
Br	2996.5	−1553.1	−1871.1	−1817.4	−1747.2	1249.3
COOMe	2997.2	−1574.5	−1871.7	−1830.0	−1758.7	1238.5
CN	2994.8	−1605.6	−1869.2	−1815.6	−1763.5	1231.4
NO_2	2994.4	−1630.8	−1867.8	−1815.7	−1771.4	1223.0
			6 (**pd**)			
H	2995.1	−1887.5	−1527.4	−1815.6	−1743.5	1251.6
NMe_2	2998.3	−1787.3	−1531.6	−1818.6	−1712.5	1285.8
OMe	3002.2	−2044.1	−1313.9	−1816.4	−1724.8	1277.4
Me	2996.4	−1843.1	−1532.7	−1814.8	−1730.2	1266.2
F	2994.8	−1851.2	−1517.7	−1815.0	−1728.0	1266.8
Cl	2995.1	−1859.5	−1519.1	−1812.1	−1730.2	1264.9
Br	2997.2	−1871.4	−1514.8	−1812.8	−1733.0	1264.2
COOMe	3003.2	−2085.4	−1341.9	−1817.2	−1748.2	1255.1
CN	2998.5	−2132.1	−1310.6	−1818.8	−1753.8	1244.6
NO_2	2995.5	−1914.6	−1502.6	−1816.1	−1744.4	1251.1

[(a)]Structures are optimized with the 6-311+G(3df) basis sets for Se and 6-311+G(3d,2p) basis sets for other nuclei at the DFT (B3LYP) level, assuming **pl** and **pd** for each of Y [47]. σ(Se) are calculated based on the DFT-GIAO method with the same methods.

Table 6: Observed $\delta(\mathrm{Se})_{\mathrm{SCS}}$ reported for **5**–**9**.

Compd	NMe_2 (**b**)	OMe (**c**)	Me (**d**)	H (**a**)	F (**e**)	Cl (**f**)	Br (**g**)	CO_2R[(a)] (**h**)	CN (**i**)	NO_2 (**j**)
5[(b)]	−20.8	−10.4	−7.2	0.0 (207.8)	—	2.5	2.8	20.1	—	33.4
5[(c)]	—	−12.5	−5.9	0.0 (202.0)	−2.0	1.6	—	16.1	—	31.4
6[(b)]	—	−15.5	−8.6	0.0 (423.6)	—	−1.7	−1.3	9.7	—	22.7
7[(d)]	−18.6	−12.6	−7.1	0.0 (641.5)	−7.1	−4.5	−4.1	0.8	8.9	4.2
8[(e)]	—	−12.0	−7.8	0.0 (320.8)	−2.5	0.2	0.9	8.6	21.0	18.0
9[(f)]	—	−9.8	−6.6	0.0 (434.3)	—	−2.7	−1.9	8.1	—	19.6

[(a)]R = Me for **5** and R = Et for **6**–**9**. [(b)]Reference [19]. [(c)]Reference [11] at neat. [(d)]Reference [13]. [(e)]Reference [8]. [(f)]Reference [15, 16].

of $4p_z$(Se) in n_p(Se) with $4p_x$(Se) and $4p_y$(Se) in modified σ^*(CSeX) since n_p(Se) of $4p_z$(Se) is filled with electrons. Therefore, Y of both donors and acceptors are effective in **pl**, whereas Y of donors are more effective in **pd**. The expectations are just observed in **1** and **2**. Sets of δ(Se: **1**) and δ(Se: **2**) can be used as the standards for **pl** and **pd**, respectively, when δ(Se) of aryl selenides are analyzed.

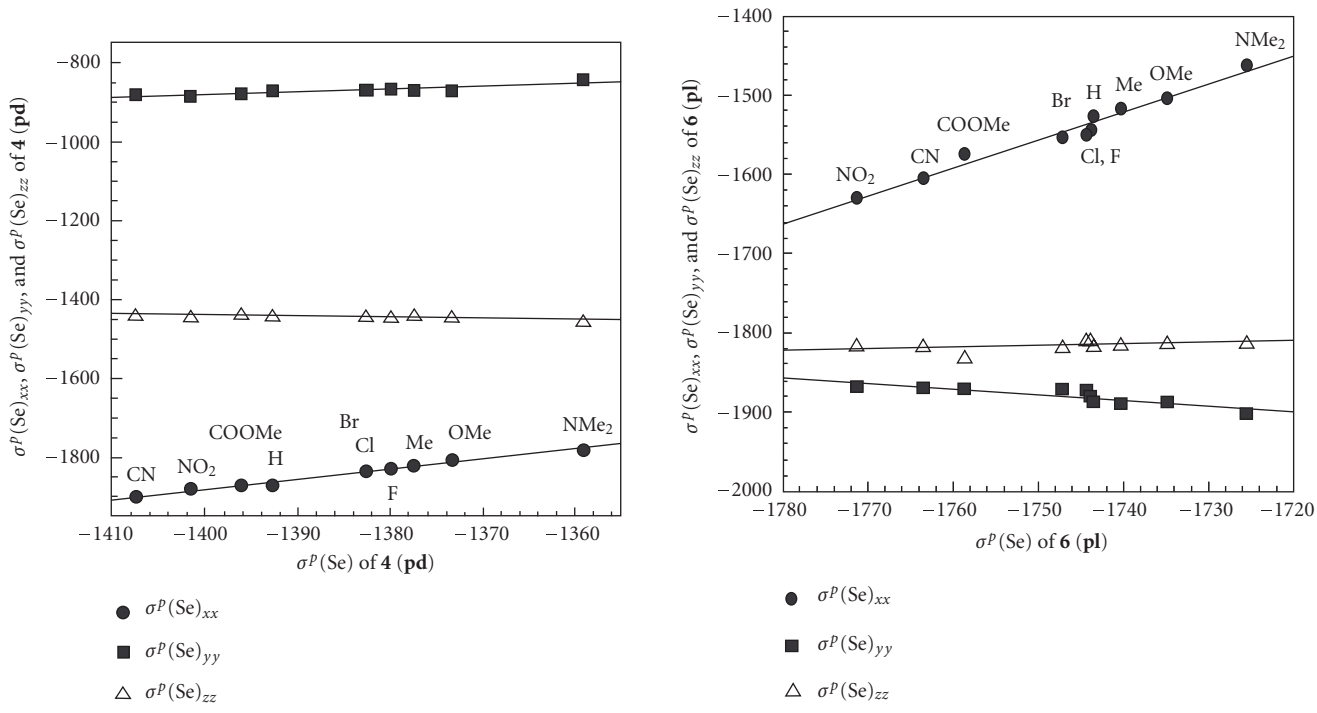

Figure 3: Plots of $\sigma^p(Se)_{xx}$ (●), $\sigma^p(Se)_{yy}$ (■), and $\sigma^p(Se)_{zz}$ (△) versus $\sigma^p(Se)$: (a) for **4** (**pd**) and (b) for **6** (**pl**).

The effect of R in ArSeR is also important, which is in progress. The results will be discussed elsewhere, together with the applications of the method.

EXPERIMENTAL

NMR spectra were recorded at 25°C on a JEOL JNM-AL 300 spectrometer (^{1}H, 300 MHz; ^{13}C, 75.45 MHz; ^{77}Se, 57.25 MHz). The ^{1}H, ^{13}C, and ^{77}Se chemical shifts are given in parts per million relative to those of Me_4Si, internal $CDCl_3$ in the solvent, and external MeSeMe, respectively.

Preparation of compounds

1a–1j were prepared by the reactions of anthracenylgrignard reagents with arylselanylbromides and/or aromatic diazonium salts with anthracenylselenolates as the case of **3** [14]. **2a–2j** were prepared by the reactions of 8-chloroanthraquione and arylselenolates with CuI as described earlier [51]. Elementary analyses for the compounds were satisfactory to those calculated within ±0.3% accuracy. ^{1}H, ^{13}C, and ^{77}Se NMR chemical shifts of the compounds rationalize the structures.

MO calculations

Quantum chemical (QC) calculations were performed using a Silent-SCC T2 (Itanium2) computer with the 6-311+G(3df) basis sets for Se and 6-311+G(3d,2p) for other nuclei of the Gaussian 03 program [47]. Calculations are performed on **4–6** in **pl** and **pd** at the density functional theory (DFT) level of the Becke three parameter hybrid functionals combined with the Lee-Yang-Parr correlation functional (B3LYP). Absolute magnetic shielding tensors of Se nuclei (σ(Se)) are calculated based on the gauge-independent atomic orbital (GIAO) method, applying on the optimized structures with the same method.

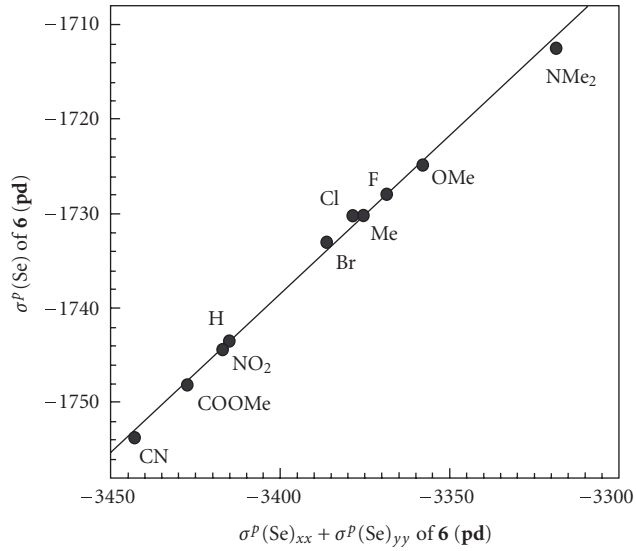

Figure 4: Plot of σ^p(Se) versus $\sigma^p(Se)_{xx} + \sigma^p(Se)_{yy}$ for **6** (**pd**).

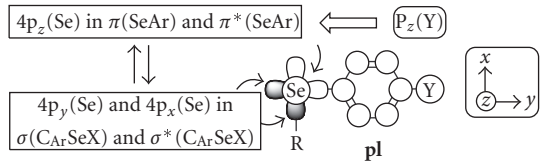

Main interaction between Y and Se in **pl**: 4p$_z$(Se)-π(C$_6$H$_4$)-p$_z$(Y). Main origin of Y dependence in **pl**: admixtures between 4p$_z$(Se) in π(SeAr) and (4p$_x$(Se), 4p$_y$(Se)) in σ^*(C$_{Ar}$SeX) and 4p$_z$(Se) in π^*(SeAr) and (4p$_x$(Se), 4p$_y$(Se)) in σ(C$_{Ar}$SeX)

(a)

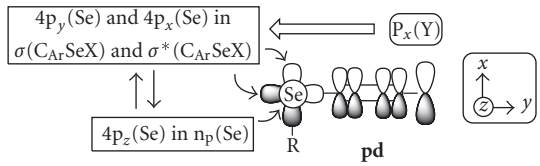

Main interaction between Y and Se in **pd**: σ(C$_{Ar}$SeX)-π(C$_6$H$_4$)-p$_x$(Y). Main origin of Y dependence in **pd**: admixtures between 4p$_z$(Se) in n$_p$(Se) and (4p$_x$(Se), 4p$_y$(Se)) in σ^*(CSeX)

(b)

Scheme 3: Mechanisms of Y dependence. Outline allows exhibit the effect of p(Y) on 4p(Se) and double allows show the main admixtures to originate δ(Se): (a) in **pl** and (b) in **pd**.

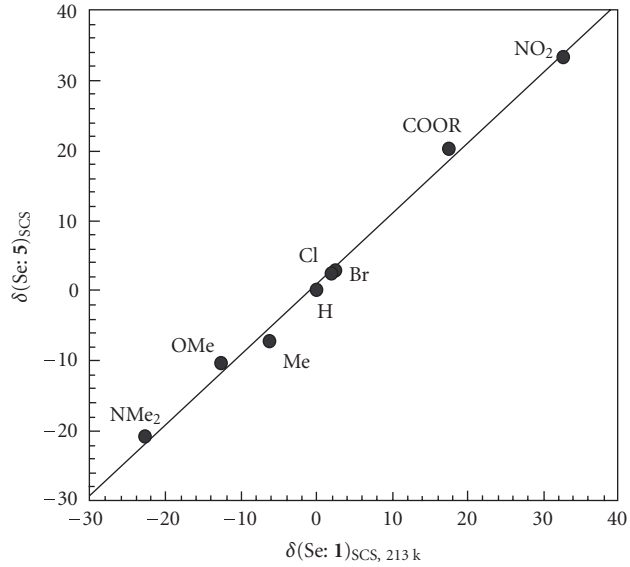

Figure 5: Plot of δ(Se: **5**)$_{SCS}$ versus δ(Se: **1**)$_{SCS,\ 213\,K}$.

Structures of **1a**–**3a** in various conformers are also optimized, containing frequency analysis, with the B3LYP/6-311+G(d,p) method.

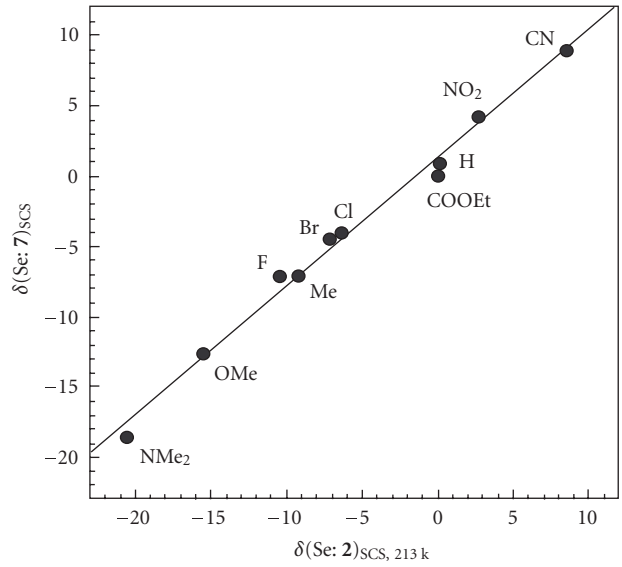

Figure 6: Plot of δ(Se: **7**)$_{SCS}$ versus δ(Se: **2**)$_{SCS,\ 213\,K}$.

ACKNOWLEDGMENT

This work was partially supported by a Grant-in-Aid for Scientific Research (no 16550038) from the Ministry of Education, Culture, Sports, Science, and Technology, Japan.

REFERENCES

[1] Klayman DL, Günther WHH, eds. *Organic Selenium Compounds: Their Chemistry and Biology.* New York, NY: John Wiley & Sons; 1973.

[2] Patai S, Rappoport Z, eds. *The Chemistry of Organic Selenium and Tellurium Compounds.* Vol 1 and 2. New York, NY: John Wiley & Sons; 1986.

[3] Liotta D, ed. *Organic Selenium Chemistry.* New York, NY: Wiley-Interscience; 1987.

[4] Back TG, ed. *Organoselenium Chemistry, A practical Approach.* Oxford, Uk: Oxford University Press; 1999.

[5] Wirth T, ed. *Organoselenium Chemistry: Modern Developments in Organic Synthesis.* Berlin, Germany: Springer; 2000. Top. Curr. Chem.; vol 208.

[6] MacFarlane W, Wood RJ. Nuclear magnetic double-resonance studies of organo-selenium compounds. *Journal of Chemical Society, Dalton Transactions.* 1972;13:1397–1401.

[7] Iwamura H, Nakanishi W. Recent application of of ^{77}Se NMR spectroscopy in organoselenium chemistry. *Journal of Synthetic Organic Chemistry Japan.* 1981;39:795–804.

[8] Patai S, Rappoport Z, eds. *The Chemistry of Organic Selenium and Tellurium Compounds, Vol. 1.* Chapter 6. New York, NY: John Wiley & Sons; 1986.

[9] Klapotke TM, Broschag M, eds. *Compilation of Reported ^{77}Se NMR Chemical Shifts.* New York, NY: John Wiley & Sons; 1996.

[10] Duddeck H. Selenium-77 nuclear magnetic resonance spectroscopy. *Progress in Nuclear Magnetic Resonance Spectroscopy.* 1995;27(1–3):1–323.

[11] Kalabin GA, Kushnarev DF, Bzesovsky VM, Tschmutova GA. ^{1}H, ^{13}C and ^{77}Se NMR spectra of substituted selenoanisoles. *Journal of Organic Magnetic Resonance.* 1979;12(10):598–604.

[12] Kalabin GA, Kushnarev DF, Mannafov TG. NMR spectroscopy of selenium and tellurium organic compounds. III. parameters of proton, carbon-13, and selenium-77 spectra and structure of gem-dichlorocytopropylaryl selenides. *Zhurnal Organicheskoi Khimii.* 1980;16:505–512.

[13] Mullen GP, Luthra NP, Dunlap RB, Odom JD. Synthesis and multinuclear magnetic resonance study of para-substituted phenyl selenobenzoates. *The Journal of Organic Chemistry.* 1985;50(6):811–816.

[14] Nakanishi W, Hayashi S, Uehara T. Structure of 1-(Arylselanyl)naphthalenes - Y dependence in $1-(p-YC_6H_4Se)C_{10}H_7$. *European Journal of Organic Chemistry.* 2001;2001(20): 3933–3943.

[15] Hayashi S, Nakanishi W. Novel substituent effect on ^{77}Se NMR chemical shifts caused by 4c-6e versus 2c-4e and 3c-4e in naphthalene peri positions: spectroscopic and theoretical study. *The Journal of Organic Chemistry.* 1999;64(18):6688–6696.

[16] Nakanishi W, Hayashi S, Yamaguchi H. Inverse substituent effect on ^{77}Se NMR chemical shifts in naphthalene systems with linear 4c-6e Se_4 Bond: $1-[8-(p-YC_6H_4Se)C_{10}H_6]SeSe[C_{10}H_6(SeC_6H_4Y-p)\text{-}8']-1'$ *vs.* $1-(MeSe)-8-(p-YC_6H_4Se)C_{10}H_6$. *Chemistry Letters.* s1996;25(11):947–948.

[17] Nakanishi W, Hayashi S, Sakaue A, Ono G, Kawada Y. Attractive interaction caused by the linear $F\cdots Se-C$ alignment in naphthalene peri positions. *Journal of the American Chemical Society.* 1998;120(15):3635–3640.

[18] Nakanishi W, Hayashi S. Structure of 1-(Arylselanyl)naphthalenes. 2. G dependence in $8-G-1-(p-YC_6H_4Se)C_{10}H_6$. *The Journal of Organic Chemistry.* 2002;67(1):38–48.

[19] Nakanishi W, Hayashi S. On the factors to determine ^{77}Se NMR chemical shifts of organic selenium compounds: application of GIAO magnetic schielding tensor to the ^{77}Se NMR spectroscopy. *Chemistry Letters.* 1998;27(6):523–524.

[20] Nakanishi W, Hayashi S. Structural study of Aryl selenides in solution based on ^{77}Se NMR chemical shifts: application of the GIAO magnetic shielding tensor of the ^{77}Se nucleus. *The Journal of Physical Chemistry A.* 1999;103(31):6074–6081.

[21] Sitkoff D, Gase DA. Density functional calculations of proton chemical shifts in model peptides. *Journal of the American Chemical Society.* 1997;119(50):12262–12273.

[22] Xu XP, Gase DA. Probing multiple effects on ^{15}N, $^{13}C\alpha$, $^{13}C\beta$ and $^{13}C'$ chemical shifts in peptides using density functional theory. *Biopolymers.* 2002;65(6):408–423.

[23] Wishart DS, Gase DA. Use of chemical shifts in macromolecular structure determination. *Methods Enzymol.* 2001;338:3–34.

[24] Xu XP, Gase DA. Automated prediction of ^{15}N, $^{13}C\alpha$, $^{13}C\beta$ and $^{13}C'$ chemical shifts in proteins using a density functional database. *Journal of Biomolecular NMR.* 2001;21(4):321–333.

[25] Nakanishi W, Hayashi S, Shimizu D, Hada M. Orientational effect of Aryl groups on ^{77}Se NMR chemical shifts: experimental and theoretical investigations. *Chemistry—A European Journal.* 2006;12(14):3829–3846.

[26] Nakanishi W, Hayashi S, Uehara T. Successive change in conformation caused by *p*-Y groups in $1-(MeSe)-8-(p-YC_6H_4Se)C_{10}H_6$: role of linear $Se\cdots Se$-C three-center-four-electron versus $n(Se)\cdots n(Se)$ two-center-four-electron nonbonded interactions. *The Journal of Physical Chemistry A.* 1999;103(48):9906–9912.

[27] Bordwen K, Grubbs EJ. Angular dependence of dipolar substituent effects. In: Taft RW, ed. *Progress in Physical Organic Chemistry.* Vol 19. New York, NY: John Wiley & Sons; 1993:183–224.

[28] Fukuda R, Hada M, Nakatsuji H. Quasirelativistic theory for the magnetic shielding constant. I. Formulation of Douglas-Kroll-Hess transformation for the magnetic field and its application to atomic systems. *The Journal of Chemical Physics.* 2003;118(3):1015–1026.

[29] Fukuda R, Hada M, Nakatsuji H. Quasirelativistic theory for magnetic shielding constants. II. Gauge-including atomic orbitals and applications to molecules. *The Journal of Chemical Physics.* 2003;118(3):1027–1035.

[30] Tanaka S, Sugimoto M, Takashima H, Hada M, Nakatsuji H. Theoretical study on metal NMR chemical shifts. Electronic mechanism of the Xe chemical shift. *Bulletin of the Chemical Society of Japan.* 1996;69(4):953–959.

[31] Ballard CC, Hada M, Kaneko H, Nakatsuji H. Relativistic study of nuclear magnetic shielding constants: hydrogen halides. *Chemical Physics Letters.* 1996;254(3-4):170–178.

[32] Nakatsuji H, Hada M, Kaneko H, Ballard CC. Relativistic study of nuclear magnetic shielding constants: mercury dihalides. *Chemical Physics Letters.* 1996;255(1–3):195–202.

[33] Hada M, Kaneko H, Nakatsuji H. Relativistic study of nuclear magnetic shielding constants: tungsten hexahalides and tetraoxide. *Chemical Physics Letters.* 1996;261(1-2):7–12.

[34] Grant DM, Harris RK, eds. *Encyclopedia of Nuclear Magnetic Resonance.* New York, NY: John Wiley & Sons; 1996.

[35] Tossell JA, ed. *Nuclear Magnetic Shieldings and Molecular Structure.* Dordrecht, The Netherlands: Kluwer Academic; 1993.

[36] Kaupp M, Bühl M, Malkin VG, eds. *Calculation of NMR and EPR Parameters: Theory and Applications.* Weinheim, Germany: Wiley-VCH; 2004.

[37] McWeeny R, ed. *Spins in Chemistry.* New York, NY: Academic Press; 1970.

[38] Markin VG, Malkina OL, Eriksson LA. A tool for chemistry. In: Seminario JM, Politzer P, eds. *Modern Density Functional Theory.* Amsterdam, The Netherlands: Elsevier; 1994.

[39] Springborg M, ed. *Density-Functional Methods in Chemistry and Material Science.* New York, NY: John Wiley & Sons; 1977.

[40] Kanda K, Nakatsuji H, Yonezawa T. Theoretical study of the metal chemical shift in nuclear magnetic resonance spectroscopy. Manganese complexes. *Journal of the American Chemical Society.* 1984;106(20):5888–5892.

[41] Atkins PW, Friedman RS, eds. *Molecular Quantum Mechanics.* 3rd ed. Chapter 13. Oxford, NY: Oxford University Press; 1997.

[42] Wolinski K, Hinton JF, Pulay P. Efficient implementation of the gauge-independent atomic orbital method for NMR chemical shift calculations. *Journal of the American Chemical Society.* 1990;112(23):8251–8260.

[43] Wolinski K, Sadlej A. Self-consistent perturbation theory. Open-shell states in perturbation-dependent non-orthogonal basis sets. *Molecular Physics.* 1980;41(6):1419–1430.

[44] Ditchfield R. Self-consistent perturbation theory of diamagnetism. I. A gauge-invariant LCAO method for NMR chemical shifts. *Molecular Physics.* 1974;27(4):789–807.

[45] McWeeny R. Perturbation theory for the fock-dirac density matrix. *Physical Review.* 1962;126(3):1028–1034.

[46] London F. Théorie quantique des courants interatomiques dans les combinaisons aromatiques. *Journal de Physique et le Radium.* 1937;8:397–409.

[47] Frisch MJ, Trucks GW, Schlegel HB, et al. *Gaussian 03 (Revision B.05).* Pittsburgh, Pa: Gaussian; 2003.

[48] Wilson PJ. Accurate non-relativistic density functional theory predictions for ^{77}Se NMR shielding parameters. *Molecular Physics.* 2001;99(4):363–367.

[49] Ramsey NF. Magnetic shielding of nuclei in molecules. *Physical Review.* 1950;78(5):699–703.

[50] Nakanishi W. Hypervalent chalcogen compounds. In: Devillanova FA, ed. *Handbook of Chalcogen Chemistry, New Perspectives in Sulfur, Selenium and Tellurium.* Chapter 10.3. London, UK: Royal Society of Chemistry; 2006.

[51] Nakanishi W, Hayashi S, Itoh N. Extended hypervalent 5c-6e interactions: linear alignment of five C-Se—O—Se-C atoms in anthraquinone and 9-methoxyanthracene bearing Arylselanyl groups at the 1,8-positions. *The Journal of Organic Chemistry.* 2004;69(5):1676–1684.